

# Doubly Dispersive Channel Estimation with Scalable Complexity

Michal Šimko, Christian Mehlführer, Martin Wrulich and Markus Rupp

Institute of Communications and Radio-Frequency Engineering, Vienna University of Technology

Gusshausstrasse 25/389, A-1040 Vienna, Austria

Email: {msimko, chmehl, mwrulich, mrupp}@nt.tuwien.ac.at

Web: <http://www.nt.tuwien.ac.at/rapid-prototyping>

**Abstract**—In this paper, we present an **Approximate Linear Minimum Mean Square Error (ALMMSE) fast fading channel estimator for Orthogonal Frequency Division Multiplexing (OFDM)**. The ALMMSE channel estimator utilizes the knowledge of the structure of the autocorrelation matrix given by the Kronecker product between the time correlation matrix and the frequency correlation matrix. We separate the Linear Minimum Mean Square Error (LMMSE) filtering matrix into two matrices corresponding to individual filtering in frequency and time. The eigenvalues of these two matrices are rank-one approximated by the eigenvalues of the LMMSE filtering matrix. The complexity of the ALMMSE estimator can be scaled by varying the number of the considered number of eigenvalues. Simulation results show that the proposed ALMMSE channel estimator loses only 0.1 dB compared to the LMMSE channel estimator in realistic scenarios.

**Index Terms**—LTE, Channel Estimation, Fast Fading, OFDM.

## I. INTRODUCTION

An essential part of modern wireless communications receivers is the channel estimator whose quality has a direct impact on the data throughput. The complexity and implementation of a channel estimator strongly depends on the statistics of the channel, in particular the coherence time. With a coherence time longer than the typical transmission timing interval, the channel appears as a block fading. In this case it is sufficient to estimate the channel only once per transmission block. On the other hand, if the coherence time is smaller than the typical transmission timing interval, the channel appears as fast fading channel. Accordingly, the channel estimation has to adapt to this circumstance.

The channel estimation for Orthogonal Frequency Division Multiplexing (OFDM) systems in case of block fading [1–4] is a well studied topic for certain pilot symbol structures. Exemplary estimator classes are the Least Squares (LS) and the Linear Minimum Mean Square Error (LMMSE) channel estimators, which for example have also been applied in Long Term Evolution (LTE) for Universal Mobile Telecommunications System (UMTS) [5]. Today's wireless communication systems however are designed to provide high data rates also to mobile users. The channel of a quickly moving user is changing rapidly during a subframe, rendering the channel coherence time small. Consequently, the utilization of block

fading channel estimators would result in a significant performance loss. A suitable estimator in a fast fading environment is the LMMSE fast fading channel estimator [6–8], which however suffers from high computational complexity. Furthermore, the complexity of the proposed channel estimators is fixed, independent of the actual requirements. In this work we discuss the performance of the standard channel estimators in case of the fast fading for LTE using the 3rd Generation Partnership Project (3GPP) standardized pilot symbol pattern. Furthermore, we propose an approximation of the LMMSE fast fading channel estimator with scalable complexity, which we call *Approximate Linear Minimum Mean Square Error (ALMMSE) estimator*.

The paper is organized as follows. In Section II we describe the pilot symbol structure of the LTE standard and the mathematical system model. State-of-the-art channel estimator, such as the LS for block fading, the LS for fast fading and the LMMSE for fast fading, are presented in Section III. We introduce our ALMMSE fast fading channel estimator in Section IV. In Section V we evaluate the performance of the explained channel estimators in terms of physical layer data throughput and Mean Square Error (MSE). Finally, we conclude the paper in Section VI.

## II. SYSTEM MODEL

In this section, the structure of the pilot symbols for 3GPP LTE is described. In the time domain, the LTE signal consists of frames with a duration of  $T_{\text{frame}} = 10$  ms. Each frame is split into ten equally long subframes and each subframe into two equally long slots with a duration of  $T_{\text{slot}} = 0.5$  ms. Depending on the cyclic prefix length, being either extended or normal, each slot consists of  $N_s = 6$  or  $N_s = 7$  OFDM symbols, respectively. In LTE, the subcarrier spacing is fixed to 15 kHz. Twelve adjacent subcarriers of one slot are grouped into a so-called resource block. The number of resource blocks in an LTE slot ranges from 6 up to 100, corresponding to a bandwidth from 1.4 MHz up to 20 MHz.

The positions of the pilot symbols in the time-frequency grid depend on the number of transmit antenna ports [9]. Whenever there is a pilot symbol located within the time-frequency grid at one transmit antenna port, this position on the remaining transmit antenna ports is not used. We call the

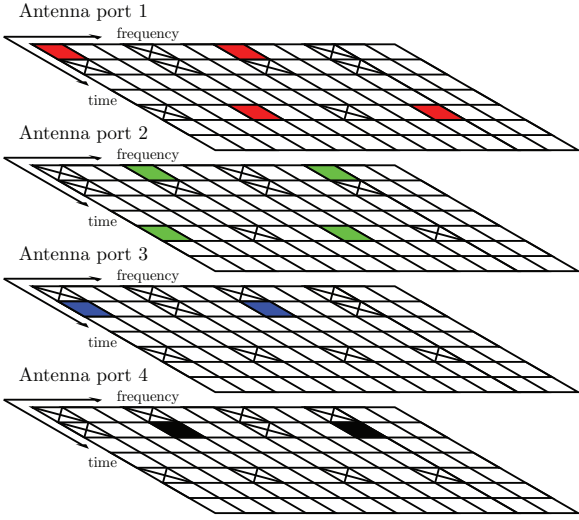


Fig. 1. Structure of the pilot symbols within one resource block if four transmit antenna ports and normal cyclic prefix are employed

corresponding symbols *zero-symbols* in the following. Figure 1 depicts the structure of the pilot symbols within one resource block if four transmit antenna ports and normal cyclic prefix are employed. The colored squares correspond to the pilot symbols at a particular antenna port and crosses correspond to the zero-symbols. Each resource block at the 1st and the 2nd transmit antenna port contains four pilot symbols. At the 3rd and 4th transmit antenna port just two pilot symbols are available per resource block. It is obvious that with increasing number of antenna ports, the overhead for pilot symbols and zero-symbols is increasing. This fact results in decreasing spectral efficiency with increasing number of transmit antenna ports; that is, in case of four transmit antenna ports 14.3% of all symbols are reserved just for channel estimation. The applied pilot symbol pattern allows to estimate a Multiple Input Multiple Output (MIMO) channel as independent Single Input Single Output (SISO) channels, if spatial correlation is neglected or assumed to be low.

The  $n$ -th received OFDM symbol  $\mathbf{y}_n$  at one receive antenna port can be written as

$$\mathbf{y}_n = \mathbf{X}_n \mathbf{h}_n + \mathbf{w}_n, \quad (1)$$

where the vector  $\mathbf{h}_n$  contains the channel coefficients in the frequency domain and  $\mathbf{w}_n$  is additive white zero mean Gaussian noise with variance  $\sigma_w^2$ . The diagonal matrix  $\mathbf{X}_n = \text{diag}(\mathbf{x}_n)$  comprises the data symbols  $\mathbf{x}_{d,n}$  and the pilot symbols  $\mathbf{x}_{p,n}$  permuted by a permutation matrix  $\mathbf{P}$  on the main diagonal

$$\mathbf{x}_n = \mathbf{P} [\mathbf{x}_{p,n}^T \mathbf{x}_{d,n}^T]^T. \quad (2)$$

The length of the vector  $\mathbf{x}_n$  is  $K$  corresponding to the number of subcarriers. Note that according to Equation (2), also the vectors  $\mathbf{y}_n$ ,  $\mathbf{h}_n$  and  $\mathbf{w}_n$  can be divided into two parts corresponding to the pilot symbol positions and to the data symbol positions.

### III. STATE-OF-THE-ART CHANNEL ESTIMATION

In this section, we present three typical state-of-the-art channel estimators that are used as a benchmark for our novel ALMMSE channel estimator introduced in the next section.

#### A. LS Channel Estimation

The LS channel estimator [1] for the pilot symbol positions is given as the solution to the minimization problem

$$\hat{\mathbf{h}}_p^{\text{LS}} = \arg \min_{\hat{\mathbf{h}}_p} \left\| \mathbf{y}_p - \mathbf{X}_p \hat{\mathbf{h}}_p \right\|_2^2 = \mathbf{X}_p^{-1} \mathbf{y}_p. \quad (3)$$

At the non-pilot symbol positions, the remaining channel coefficients have to be obtained by two dimensional interpolation. In this work, we use linear interpolation. The LS channel estimator does not require knowledge about the channel and noise statistics and can be implemented with low complexity.

In case block fading is assumed, the LS channel estimator can be simplified even further. First, the channel estimates for time-frequency grid positions with pilot symbols are calculated by using Equation (3). Utilizing the assumption that the channel stays constant during the transmission of one subframe, the pilot positions channel estimates at different points in time can be averaged. The remaining channel coefficients in the frequency domain then have to be obtained by only one dimensional interpolation. In this work, we use linear interpolation.

#### B. LMMSE Channel Estimation

The LMMSE channel estimator requires the second order statistics of the channel and the noise. It can be shown that the LMMSE channel estimate is obtained by multiplying the LS estimate with a filtering matrix  $\mathbf{A}_{\text{LMMSE}}$  [5]

$$\hat{\mathbf{h}}_{\text{LMMSE}} = \mathbf{A}_{\text{LMMSE}} \hat{\mathbf{h}}_p^{\text{LS}}. \quad (4)$$

In order to find the LMMSE filtering matrix, the MSE

$$\epsilon = \mathbb{E} \left\{ \left\| \mathbf{h} - \mathbf{A}_{\text{LMMSE}} \hat{\mathbf{h}}_p^{\text{LS}} \right\|_2^2 \right\}, \quad (5)$$

has to be minimized, leading to

$$\mathbf{A}_{\text{LMMSE}} = \mathbf{R}_{\mathbf{h}, \mathbf{h}_p} (\mathbf{R}_{\mathbf{h}_p, \mathbf{h}_p} + \sigma_w^2 \mathbf{I})^{-1}, \quad (6)$$

where the matrix  $\mathbf{R}_{\mathbf{h}_p, \mathbf{h}_p} = \mathbb{E} \{ \mathbf{h}_p \mathbf{h}_p^H \}$  is the channel autocorrelation matrix at the pilot symbols, and the matrix  $\mathbf{R}_{\mathbf{h}, \mathbf{h}_p} = \mathbb{E} \{ \mathbf{h} \mathbf{h}_p^H \}$  is the channel crosscorrelation matrix.

### IV. ALMMSE CHANNEL ESTIMATION

In the following section, we present a novel fast fading channel estimator, which approximates the LMMSE channel estimator. The main idea is to make use of the structure of the channel autocorrelation matrix, assumed to be given by

$$\mathbf{R}_{\mathbf{h}} \triangleq \mathbf{R}_{\text{time}} \otimes \mathbf{R}_{\text{freq}}, \quad (7)$$

where  $\mathbf{R}_{\text{time}}$  is the time correlation matrix and  $\mathbf{R}_{\text{freq}}$  is the frequency correlation matrix. The Kronecker structure assumption of the channel autocorrelation matrix  $\mathbf{R}_{\mathbf{h}}$  corresponds to independent time- and frequency-correlation.

The standard LMMSE estimate is obtained by minimizing the error in Equation (5). Let us consider the following problem instead

$$\min_{\mathbf{B}_{\text{freq}}, \mathbf{C}_{\text{time}}} \mathbb{E} \left\{ \|\mathbf{H} - \mathbf{B}_{\text{freq}} \hat{\mathbf{H}}_{\text{LS}} \mathbf{C}_{\text{time}}^{\text{T}}\|_{\text{F}}^2 \right\}, \quad (8)$$

with the channel  $\mathbf{H} = [\mathbf{h}_0, \dots, \mathbf{h}_{N_s-1}]$  and the LS channel estimate  $\hat{\mathbf{H}}_{\text{LS}} = [\hat{\mathbf{h}}_0^{\text{LS}}, \dots, \hat{\mathbf{h}}_{N_s-1}^{\text{LS}}]$ . Here,  $N_s$  denotes the number of OFDM symbols,  $\mathbf{B}_{\text{freq}}$  and  $\mathbf{C}_{\text{time}}$  are matrices of dimension  $K \times K$  and  $N_s \times N_s$ , respectively.  $\|\cdot\|_{\text{F}}$  refers to the Frobenius norm. The approach in Equation (8) corresponds to a separate filtering of the LS estimate in time and frequency. After applying the  $\text{vec}(\cdot)$  operator [10] in Equation (8) by using  $\mathbf{h} = \text{vec}(\mathbf{H})$ ,  $\hat{\mathbf{h}}_{\text{LS}} = \text{vec}(\hat{\mathbf{H}}_{\text{LS}})$ , and

$$\text{vec}(\mathbf{B}_{\text{freq}} \hat{\mathbf{H}}_{\text{LS}} \mathbf{C}_{\text{time}}^{\text{T}}) = (\mathbf{C}_{\text{time}} \otimes \mathbf{B}_{\text{freq}}) \text{vec}(\hat{\mathbf{H}}_{\text{LS}}), \quad (9)$$

we obtain

$$\min_{\mathbf{B}_{\text{freq}}, \mathbf{C}_{\text{time}}} \mathbb{E} \left\{ \|\mathbf{h} - (\mathbf{C}_{\text{time}} \otimes \mathbf{B}_{\text{freq}}) \hat{\mathbf{h}}_{\text{LS}}\|_2^2 \right\}. \quad (10)$$

The problems formulated in Equation (5) and Equation (10) are equivalent. However, in general  $\mathbf{A}_{\text{LMMSE}}$  cannot always be decomposed into  $\mathbf{C}_{\text{time}} \otimes \mathbf{B}_{\text{freq}}$ . Instead, we are searching for the best approximation

$$\mathbf{A}_{\text{LMMSE}} \approx \mathbf{C}_{\text{time}} \otimes \mathbf{B}_{\text{freq}}. \quad (11)$$

Due to the pilot symbols pattern utilized in LTE, that is not equidistant in the time and frequency, the structure from Equation (7) cannot be exploited in  $\mathbf{R}_{\mathbf{h}_p, \mathbf{h}_p}$  and  $\mathbf{R}_{\mathbf{h}, \mathbf{h}_p}$ . Therefore, we replace the auto- and crosscorrelation matrices in Equation (6) by the channel autocorrelation matrix  $\mathbf{R}_{\mathbf{h}}$ . Therefore, instead of filtering the LS estimate at the pilot symbols position, the interpolated LS estimate has to be filtered. The dimension of filtering matrix in Equation (6) is changed from  $KN_s \times N_p$  to  $KN_s \times KN_s$ , where  $N_p$  is the number of the pilot symbols. In the Signal to Noise Ratio (SNR) range of interest, such an estimator performs close to the true LMMSE channel estimator. For pilot symbol pattern that is equidistant in time frequency, the structure from Equation (7) can be exploited. Using Equations (6) and (7), the matrix  $\mathbf{A}_{\text{LMMSE}}$  is given by

$$\mathbf{A}_{\text{LMMSE}} = \mathbf{R}_{\text{time}} \otimes \mathbf{R}_{\text{freq}} (\mathbf{R}_{\text{time}} \otimes \mathbf{R}_{\text{freq}} + \sigma_w^2 \mathbf{I})^{-1}. \quad (12)$$

The symmetric matrices  $\mathbf{R}_{\text{time}}$  and  $\mathbf{R}_{\text{freq}}$  can be rewritten using the eigenvalue decomposition as

$$\mathbf{R}_{\text{time}} = \mathbf{U}_{\text{time}} \mathbf{D}_{\text{time}} \mathbf{U}_{\text{time}}^{\text{H}}, \quad \mathbf{R}_{\text{freq}} = \mathbf{U}_{\text{freq}} \mathbf{D}_{\text{freq}} \mathbf{U}_{\text{freq}}^{\text{H}},$$

where  $\mathbf{D}_{\text{time}}$  and  $\mathbf{D}_{\text{freq}}$  are diagonal matrices, with their corresponding eigenvalues ordered from largest to smallest on the main diagonal.  $\mathbf{U}_{\text{time}}$  and  $\mathbf{U}_{\text{freq}}$  are unitary matrices comprising the eigenvectors of the given matrices. Furthermore, due to the Kronecker product properties, one can write

$$\mathbf{R}_{\text{time}} \otimes \mathbf{R}_{\text{freq}} = (\mathbf{U}_{\text{time}} \otimes \mathbf{U}_{\text{freq}}) \mathbf{D}_{\mathbf{h}} (\mathbf{U}_{\text{time}} \otimes \mathbf{U}_{\text{freq}})^{\text{H}},$$

where  $\mathbf{D}_{\mathbf{h}}$  is a diagonal matrix with eigenvalues of the matrix  $\mathbf{R}_{\text{time}} \otimes \mathbf{R}_{\text{freq}}$ , being equal to  $\mathbf{D}_{\text{time}} \otimes \mathbf{D}_{\text{freq}}$ . Inserting the last

equation into Equation (12) and after some linear algebra, the filtering matrix becomes

$$\mathbf{A}_{\text{LMMSE}} = (\mathbf{U}_{\text{time}} \otimes \mathbf{U}_{\text{freq}}) \mathbf{D}_{\mathbf{h}} (\mathbf{D}_{\mathbf{h}} + \sigma_w^2 \mathbf{I})^{-1} (\mathbf{U}_{\text{time}} \otimes \mathbf{U}_{\text{freq}})^{\text{H}}.$$

#### A. Rank-One Approximation

Let us assume that  $\mathbf{B}_{\text{freq}}$  and  $\mathbf{C}_{\text{time}}$  have the same eigenvectors as  $\mathbf{R}_{\text{freq}}$  and  $\mathbf{R}_{\text{time}}$ . Then Equation (11) can be approximated by

$$\mathbf{A}_{\text{LMMSE}} = \mathbf{U}_{\mathbf{h}} \mathbf{D}_{\mathbf{h}} (\mathbf{D}_{\mathbf{h}} + \sigma_w^2 \mathbf{I})^{-1} \mathbf{U}_{\mathbf{h}}^{\text{H}} \approx \mathbf{U}_{\mathbf{h}} \mathbf{D}_{\mathbf{C}_{\text{time}} \otimes \mathbf{B}_{\text{freq}}} \mathbf{U}_{\mathbf{h}}^{\text{H}}, \quad (13)$$

with  $\mathbf{U}_{\mathbf{h}} = \mathbf{U}_{\text{time}} \otimes \mathbf{U}_{\text{freq}}$ . The matrix  $\mathbf{D}_{\mathbf{C}_{\text{time}} \otimes \mathbf{B}_{\text{freq}}}$  is a diagonal matrix comprising the eigenvalues of the matrix  $\mathbf{C}_{\text{time}} \otimes \mathbf{B}_{\text{freq}}$ .

Moreover, let  $\lambda_{\text{time}}$ ,  $\lambda_{\text{freq}}$ ,  $\lambda_{\mathbf{C}_{\text{time}}}$  and  $\lambda_{\mathbf{B}_{\text{freq}}}$  denote the vectors of the eigenvalues of  $\mathbf{R}_{\text{time}}$ ,  $\mathbf{R}_{\text{freq}}$ ,  $\mathbf{C}_{\text{time}}$  and  $\mathbf{B}_{\text{freq}}$ , respectively. By multiplying  $\lambda_{\text{time}}$  with  $\lambda_{\text{freq}}^{\text{T}}$ , a matrix is obtained that comprises all possible multiplications of the elements of the vectors, and thus the eigenvalues of the matrix  $\mathbf{R}_{\text{time}} \otimes \mathbf{R}_{\text{freq}}$ . To solve the approximation problem  $\mathbf{D}_{\mathbf{C}_{\text{time}} \otimes \mathbf{B}_{\text{freq}}} \approx \mathbf{D}_{\mathbf{h}} (\mathbf{D}_{\mathbf{h}} + \sigma_w^2 \mathbf{I})^{-1}$ , the eigenvalues of the matrix  $\mathbf{C}_{\text{time}} \otimes \mathbf{B}_{\text{freq}}$  have to be found. Those represent all possible multiplications of the eigenvalues of the matrices  $\mathbf{C}_{\text{time}}$  and  $\mathbf{B}_{\text{freq}}$ , given by  $\lambda_{\mathbf{C}_{\text{time}}} \lambda_{\mathbf{B}_{\text{freq}}}^{\text{T}}$ . Using the matrices  $\lambda_{\text{time}} \lambda_{\text{freq}}^{\text{T}}$  and  $\lambda_{\mathbf{C}_{\text{time}}} \lambda_{\mathbf{B}_{\text{freq}}}^{\text{T}}$ , the problem can be reformulated as

$$\lambda_{\text{time}} \lambda_{\text{freq}}^{\text{T}} / (\lambda_{\text{time}} \lambda_{\text{freq}}^{\text{T}} + \sigma_w^2 \mathbf{1} \mathbf{1}^{\text{T}}) \approx \lambda_{\mathbf{C}_{\text{time}}} \lambda_{\mathbf{B}_{\text{freq}}}^{\text{T}}, \quad (14)$$

where  $\mathbf{1}$  is the all ones vector and  $/$  denotes element-wise division. This is a so-called rank-one approximation, where the best approximation is achieved when taking the left and right eigenvectors corresponding to the largest singular value, and having one of them scaled by it

$$\lambda_{\mathbf{C}_{\text{time}}} = \sigma_{\max} \mathbf{u}_{\max}, \quad (15)$$

$$\lambda_{\mathbf{B}_{\text{freq}}} = \mathbf{v}_{\max}. \quad (16)$$

Accordingly, the ALMMSE channel estimate utilizing the rank-one approximation of Equation (14) is given by

$$\hat{\mathbf{H}}_{\text{ALMMSE}} = \mathbf{B}_{\text{freq}} \hat{\mathbf{H}}_{\text{LS}} \mathbf{C}_{\text{time}}^{\text{T}}, \quad (17)$$

where the matrices  $\mathbf{B}_{\text{freq}}$  and  $\mathbf{C}_{\text{time}}$  are given by

$$\mathbf{B}_{\text{freq}} = \mathbf{U}_{\text{freq}} \text{diag}(\lambda_{\mathbf{B}_{\text{freq}}}) \mathbf{U}_{\text{freq}}^{\text{H}}, \quad (18)$$

$$\mathbf{C}_{\text{time}} = \mathbf{U}_{\text{time}} \text{diag}(\lambda_{\mathbf{C}_{\text{time}}}) \mathbf{U}_{\text{time}}^{\text{H}}. \quad (19)$$

#### B. Complexity Scaling

By utilizing the truncated Singular Value Decomposition (SVD) [11] on  $\mathbf{R}_{\text{time}}$  and  $\mathbf{R}_{\text{freq}}$ ,  $N_{\text{time}}$  and  $N_{\text{freq}}$  largest eigenvalues can be obtained, respectively. By using Equation (14), the vectors  $\lambda_{\mathbf{C}_{\text{time}}}$  and  $\lambda_{\mathbf{B}_{\text{freq}}}$  of length  $N_{\text{time}}$  and

TABLE I  
SIMULATOR SETTINGS FOR FAST FADING SIMULATIONS

Parameter	Value
Bandwidth	1.4 MHz
Number of transmit antennas	4
Number of receive antennas	2
Receiver type	SSD
Transmission mode	Open-loop spatial multiplexing
Channel type	ITU VehA [13]
CQI	10
coding rate	466/1024 = 0.455
symbol alphabet	64 QAM
number of subframes	2000

$N_{\text{freq}}$  are calculated. The matrices  $\mathbf{B}_{\text{freq}}$  and  $\mathbf{C}_{\text{time}}$  are the same as if they would be calculated by

$$\mathbf{B}_{\text{freq}} = (\mathbf{U}_{\text{freq}})_{1:N_{\text{freq}}} \text{diag}(\lambda_{\mathbf{B}_{\text{freq}}}) (\mathbf{U}_{\text{freq}})_{1:N_{\text{freq}}}^H, \quad (20)$$

$$\mathbf{C}_{\text{time}} = (\mathbf{U}_{\text{time}})_{1:N_{\text{time}}} \text{diag}(\lambda_{\mathbf{C}_{\text{time}}}) (\mathbf{U}_{\text{time}})_{1:N_{\text{time}}}^H, \quad (21)$$

where  $(\cdot)_{1:N}$  creates a matrix, which consists of the first  $N$  columns of the matrix. The main complexity is given by the truncated SVD. Therefore, by varying  $N_{\text{time}}$  and  $N_{\text{freq}}$  the complexity can be scaled according to the requirements.

## V. SIMULATION RESULTS

In this section, we present simulation results and discuss the performance of the different channel estimation techniques. All results are obtained with the LTE Link Level Simulator version "1.2r533", developed at the Vienna University of Technology [12], that can be downloaded from [www.nt.tuwien.ac.at/ltesimulator](http://www.nt.tuwien.ac.at/ltesimulator).<sup>1</sup> We also calculated the 95% confidence intervals for all simulated curves. All intervals turned out to be smaller than the size of the markers plotted in the figures. Table I presents the most important simulator settings.

The time correlated channel was generated by an implementation of the Rosa Zheng model with modifications according to [14]. We generate a time correlated channel impulse response for every sample of the baseband transmit signal. Using a time-variant convolution the output signal of the channel is calculated.

In the following simulations, we fixed  $N_{\text{freq}} = 5$  and  $N_{\text{time}} = 2$  to reduce the complexity of the ALMMSE fast fading channel estimator. In Figure 2 the throughput of the LTE system at SNR = 20 dB is plotted with different channel estimators as a function of user velocity. It can be observed that with increasing velocity the throughput is decreasing. The LMMSE estimator outperforms the remaining channel estimators. Up to a certain velocity of about  $v = 175$  km/h, the performance of the proposed ALMMSE channel estimator is close to the LMMSE estimator. After exceeding this velocity, the energy of the time correlation is spread over more than two eigenvalues, therefore the performance is suffering. However, a user is able to move 25 km/h faster while achieving the same

<sup>1</sup>All figures can be obtained by running a script file with name `LTE_sim_batch_michal_wsa_2010`

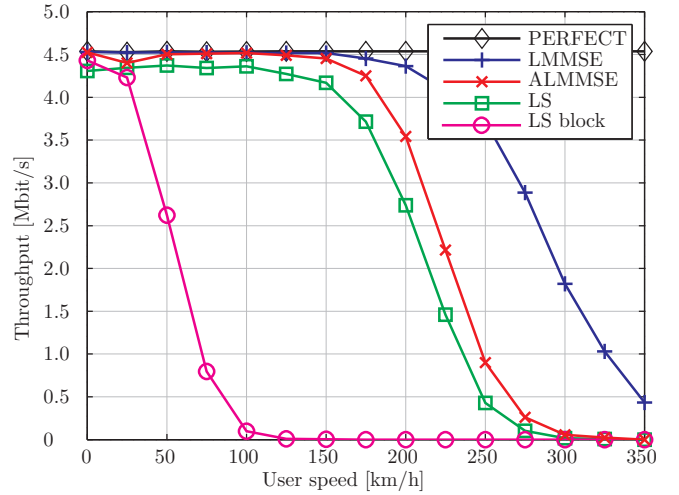


Fig. 2. Comparison of the throughput of the LTE system with different channel estimators over user velocity.

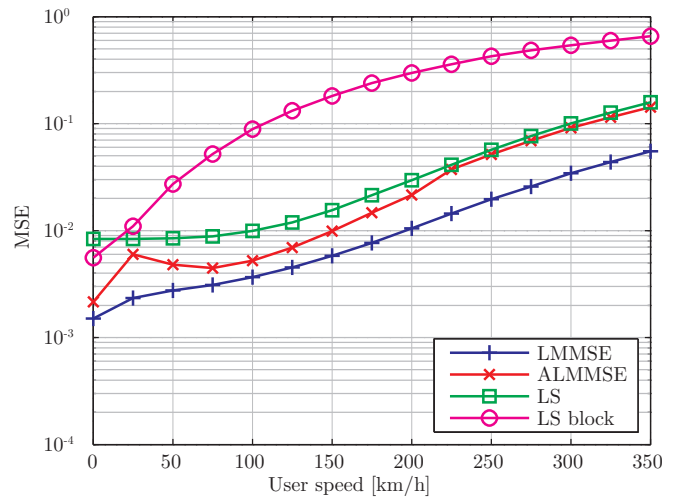


Fig. 3. Comparison of the MSE of the LTE system with different channel estimators over user velocity.

data throughput, if the ALMMSE estimator is utilized instead of the LS estimator.

When the LMMSE channel estimator is employed, the performance of the system is close to knowing the channel perfectly up to a velocity of about 150 km/h. With a further increase of the user velocity, the performance is decreasing.

Figure 3 shows the MSE for the same scenario. Up to a certain user velocity of about  $v = 20$  km/h, the MSE of the LS block fading estimator is lower than that of the LS fast fading estimator. This is because the block fading estimator inherently assumes that the channel stays constant during the transmission of one subframe and thus it performs averaging over time. At a user velocity of 25 km/h, the ALMMSE channel estimator shows a peak in the MSE which is due to numerical problems because of a small eigenvalue.

Figure 4 shows the data throughput over SNR using differ-

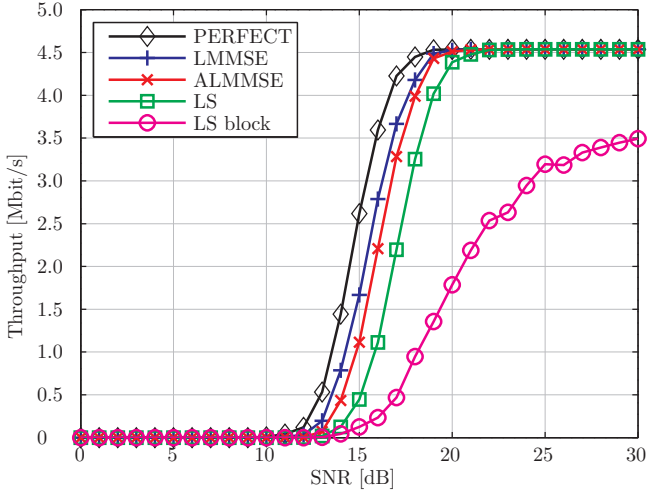


Fig. 4. Throughput of the LTE system using different channel estimators at user speed of 60 km/h.

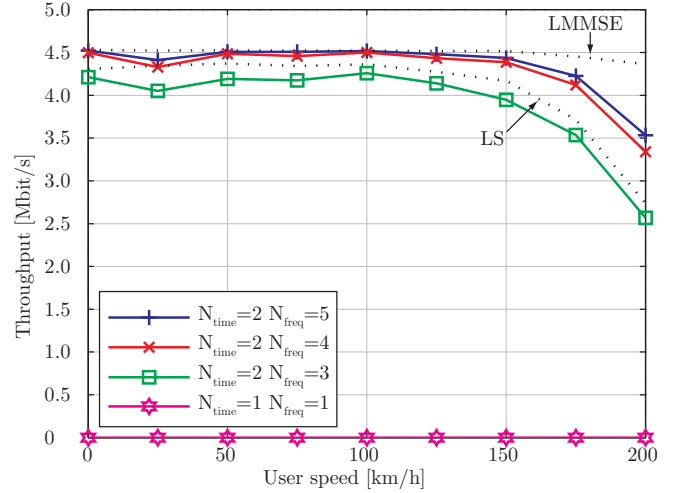


Fig. 6. Throughput of the LTE system using ALMMSE channel estimator with different number of eigenvalues over user speed

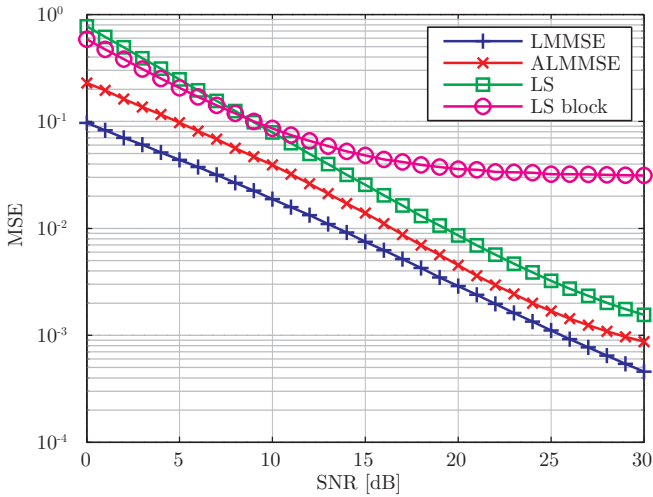


Fig. 5. Mean square error of the different channel estimators at user speed of 60 km/h

ent channel estimators. At 90% of the maximum throughput, the performance loss of the ALMMSE estimator with respect to the LMMSE estimator is approximately 0.1 dB. We measure the performance loss at 90% of the maximum throughput, because it is operating point, where the mobile operator would like to operate their systems. In the low SNR region, the LS block fading estimator slightly outperforms the LS fast fading estimator due its averaging over time, which effectively suppresses noise.

Correspondingly, Figure 5 depicts the MSE of the presented channel estimators for a user velocity of 60 km/h. With increasing SNR, the difference in MSE between the ALMMSE estimator and the LMMSE estimator, is decreasing. Furthermore, it can be observed that the MSE of the LS block fading estimator saturates. The MSE of all other channel estimators is decreasing with increasing SNR.

In Figure 6 the throughput as a function user velocity at SNR = 20 dB is depicted for the ALMMSE channel estimator using different  $N_{\text{freq}}$  and  $N_{\text{time}}$ . By varying the number of considered eigenvalues, the complexity of the ALMMSE channel estimator can be adjusted; however, also the achievable performance is affected. For the case  $N_{\text{freq}} = 1$  and  $N_{\text{time}} = 1$ , the performance is limited that much that no throughput is achieved. This is caused by ignoring large eigenvalues.

Finally, in Figure 7 we present the throughput of LTE at SNR=30 dB using  $\text{cqi}=14$  over user velocity. It can be seen, that with increasing user velocity the throughput is decreasing even with perfect channel knowledge. This is due to Inter Carrier Interference (ICI) that is not taken care of at the receiver. Under the user velocity axis, a Signal to Interference and Noise Ratio (SINR) axis is shown. It illustrate the decrease of the SINR with increasing user velocity, even though the SNR is constant. At an SNR of 20 dB, shown in Figure 2, there is no performance degradation with perfect channel knowledge with increasing velocity.

## VI. CONCLUSION

In this paper, we proposed an ALMMSE channel estimator and compared it to several state-of-the-art fast fading channel estimators. Although the MSE performance of the LS fast fading estimator is only slightly decreasing with increasing user velocity, the throughput performance is affected more dramatically. The proposed ALMMSE channel estimator is able to outperform the LS estimator and achieves a throughput performance with only 0.1 dB loss compared to the LMMSE estimator. Furthermore, the complexity of the proposed scheme can be adjusted by varying the number of considered eigenvalues, however, at the cost of estimation accuracy and consequently data throughput.

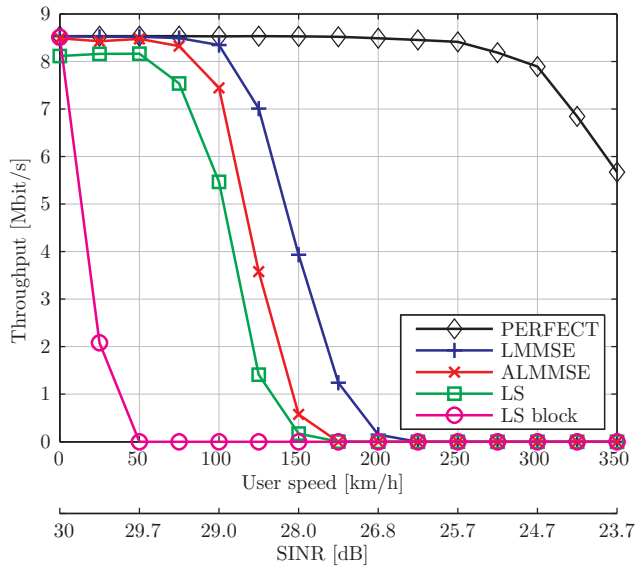


Fig. 7. Throughput of the LTE system with  $cq=14$  using different channel estimators over user speed at  $SNR=30$  dB

#### ACKNOWLEDGMENT

This work has been funded by the Christian Doppler Laboratory for Wireless Technologies for Sustainable Mobility, the Institute of Communications and Radio-Frequency Engineering, KATHREIN-Werke KG, and mobilkom austria AG.

#### REFERENCES

- [1] J. J. van de Beek, O. Edfors, M. Sandell, S. K. Wilson, and P. O. Borjesson, "On channel estimation in OFDM systems," in *Proc. IEEE 45th Vehicular Technology Conference (VTC 1995)*, 1995, vol. 2, pp. 815–819.
- [2] S. Coleri, M. Ergen, A. Puri, and A. Bahai, "Channel estimation techniques based on pilot arrangement in ofdm systems," *IEEE Transactions on Broadcasting*, vol. 48, no. 3, pp. 223–229, Sep 2002.
- [3] Ye Li, "Pilot-symbol-aided channel estimation for OFDM in wireless systems," in *1999 IEEE 49th Vehicular Technology Conference*, Jul 1999, vol. 2, pp. 1131–1135 vol.2.
- [4] Christian Mehlführer, Sebastian Caban, and Markus Rupp, "An accurate and low complex channel estimator for OFDM WiMAX," in *Proc. Third International Symposium on Communications, Control, and Signal Processing (ISCCSP 2008)*, St. Julians, Malta, Mar. 2008, pp. 922–926.
- [5] S. Omar, A. Ancora, and D.T.M. Slock, "Performance analysis of general pilot-aided linear channel estimation in LTE OFDMA systems with application to simplified MMSE schemes," in *2008. PIMRC 2008. IEEE 19th International Symposium on Personal, Indoor and Mobile Radio Communications*, Sept. 2008, pp. 1–6.
- [6] Peter Hoeher, Stefan Kaiser, and Patrick Robertson, "Pilot-symbol-aided channel estimation in time and frequency," in *In Proc. IEEE Global Telecommunications Conference (GLOBECOM 97), Communication Theory Mini-Conference*, 1997, pp. 90–96.
- [7] P. Fertl and G. Matz, "Efficient OFDM channel estimation in mobile environments based on irregular sampling," in *Proc. of Fortieth Annual Asilomar Conference on Signals, Systems, and Computers*, Pacific Grove, CA, USA, October 2006.

- [8] Won-Gyu Song and Jong-Tae Lim, "Pilot-symbol aided channel estimation for ofdm with fast fading channels," *IEEE Transactions on Broadcasting*, vol. 49, no. 4, pp. 398–402, Dec. 2003.
- [9] 3GPP, "Evolved Universal Terrestrial Radio Access (E-UTRA); Physical channels and modulation," TS 36.211, 3rd Generation Partnership Project (3GPP), Sept. 2008.
- [10] T. K. Moon and W. C. Stirling, *Mathematical Methods and Algorithms for Signal Processing*, Prentice Hall, Upper Saddle River, NJ, 2000.
- [11] Moody T. Chu, Robert E. Funderlic, and Robert J. Plemmons, "Structured low rank approximation," *Linear Algebra and its Applications*, vol. 366, pp. 157–172, 2003.
- [12] Christian Mehlführer, Martin Wrulich, Josep Colom Ikuno, Dagmar Bosanska, and Markus Rupp, "Simulating the long term evolution physical layer," in *Proc. of the 17th European Signal Processing Conference (EUSIPCO 2009)*, Glasgow, Scotland, Aug. 2009.
- [13] ITU, "Recommendation ITU-R M.1225: Guidelines for evaluation of radio transmission technologies for IMT- 2000 systems," Recommendation ITU-R M.1225, International Telecommunication Union, 1998.
- [14] T. Zemen and C.F. Mecklenbräuker, "Time-variant channel estimation using discrete prolate spheroidal sequences," *IEEE Transactions on Signal Processing*, vol. 53, no. 9, pp. 3597–3607, Sept. 2005.